AGU PUBLICATIONS

Paleoceanography

RESEARCH ARTICLE

10.1002/2014PA002744

Key Points:

- N isotope values for OAE 2 in the open ocean are never lower than −3‰
- N fixation was an important source of new N during OAE 2
- NH4 uptake by phytoplankton contributed to the low N isotopic values

Supporting Information:

- Texts S1–S4, Figures S1–S5, and Tables S1–S4

Correspondence to:
I. Ruvalcaba Baroni,
I.RuvalcabaBaroni@uu.nl

Citation:
Ruvalcaba Baroni, I., N. A. G. M. van Helmond, I. Tsandev, J. J. Middelburg, and C. P. Slomp (2015), The nitrogen isotope composition of sediments from the proto-North Atlantic during Oceanic Anoxic Event 2, *Paleoceanography*, *30*, 923–937, doi:10.1002/2014PA002744.

Received 27 OCT 2014
Accepted 5 JUN 2015
Accepted article online 9 JUN 2015
Published online 23 JUL 2015

The nitrogen isotope composition of sediments from the proto-North Atlantic during Oceanic Anoxic Event 2

I. Ruvalcaba Baroni[1], N. A. G. M. van Helmond[1], I. Tsandev[1], J. J. Middelburg[1], and C. P. Slomp[1]

[1]Department of Earth Sciences, Faculty of Geosciences, Utrecht University, Utrecht, Netherlands

Abstract Sediment records of the stable isotopic composition of N (δ^{15}N) show light δ^{15}N values at several sites in the proto-North Atlantic during Oceanic Anoxic Event 2 (OAE 2) at the Cenomanian-Turonian transition (~94 Ma). The low δ^{15}N during the event is generally attributed to an increase in N_2 fixation and incomplete uptake of NH_4^+ for phytoplankton growth. A compilation of all reliable data for the proto-North Atlantic during OAE 2 demonstrates that the most pronounced negative shift in δ^{15}N from pre-OAE 2 to OAE 2 occurs in the open ocean but with δ^{15}N never lower than −3‰. Using a box model of N cycling for the proto-North Atlantic during OAE 2, we show that N_2 fixation is a major contributor to the δ^{15}N signal, especially in the open ocean. Incomplete uptake of NH_4^+ for phytoplankton growth is important in regions dominated by downwelling, with lateral transport of NH_4^+ acting as a major source. In the southern proto-North Atlantic, where bottom waters were euxinic, the light δ^{15}N signature is largely explained by upwelling of NH_4^+. Our study provides an overview of regional differences in δ^{15}N in the proto-North Atlantic and highlights the role of lateral exchange of water and nutrients, in addition to local biogeochemical processes, in determining δ^{15}N values of OAE 2 sediments.

1. Introduction

Nitrogen (N) is an essential and often limiting nutrient for primary production in the ocean. Nitrogen fixation, a process in which certain members of the plankton community reduce atmospheric N_2 to ammonium (NH_4^+), is the major source of new N in the ocean. Although many factors may limit N_2 fixation, it is commonly favored in environments where there is a deficit of N relative to phosphorus (P) [*Gruber*, 2004]. Denitrification (here used to refer to all biological processes that remove inorganic N, including anammox [e.g., *Devol*, 2003; *Brunner et al.*, 2013]) is the major sink of fixed N in the ocean. It is largely restricted to low-oxygen zones of the water column [*Codispoti et al.*, 2001] and continental shelf and slope sediments [*Middelburg et al.*, 1996].

Global rates of denitrification and N_2 fixation can vary in time due to changes in climate and ocean oxygenation [e.g., *Algeo et al.*, 2014]. Consequently, the N inventory in the global ocean may also change with time. Because of preferential biological uptake of the lighter N isotope (^{14}N) over the heavier one (^{15}N), the N isotope composition (δ^{15}N) of bulk sediments and buried organic matter can be used to identify such perturbations of the N cycle [e.g., *Bauersachs et al.*, 2009; *Deutsch et al.*, 2004]. On the basis of δ^{15}N records, it has been suggested, for example, that water column denitrification was significantly reduced during glacial periods. This would have increased the oceanic N inventory relative to P, possibly suppressing N_2 fixation [*Ganeshram et al.*, 2002].

All biological N reactions have the potential to lead to N isotope fractionation, though the impact may vary for each process contingent on a range of factors. For example, denitrification reduces the size of the nitrite and nitrate (NO_x^-) reservoir and increases the δ^{15}N of the remaining NO_x^- pool; N_2 fixation adds N with low (slightly negative to zero) δ^{15}N to the ocean. This may counteract both the mass and isotopic effects of denitrification [*Ryabenko*, 2013]. In a system where both NH_4^+ and NO_x^- are accessible to phototrophs, NH_4^+ will be preferentially assimilated. In anoxic environments, NH_4^+ is the dominant form of N. If low-oxygen, ammonium-rich waters are upwelled, the isotope effect that results from NH_4^+ assimilation during primary production may significantly decrease δ^{15}N values of particulate organic nitrogen (PON) [*Waser et al.*, 1998; *Higgins et al.*, 2012].

Records of δ^{15}N for sediments from the proto-North Atlantic suggest a particularly strong perturbation of the N cycle during Oceanic Anoxic Event 2 (OAE 2) at the Cenomanian-Turonian transition (~94 Ma).

Table 1. Compilation of Sites Where Published and New Data of $\delta^{15}N_{TN}$ (‰) in Sediments Not Treated With Acid Are Available for the Proto-North Atlantic[a]

Site	Palaeodepth	$\delta^{15}N_{TN}$ (min, max) Pre-OAE 2	OAE 2	Shift	Reference
		Central Open Ocean			
386 (new)	~4 km	1.3 (−2.5, 2.6)	−2(−2.8, 1.1)		This study
641 (new)	~3 km	2.2 (1.8,2.7)	−0.2(−2.7, 3)		This study
1276 (new)	>2 km	1.9 (1.1,2.8)	−1.1(−2.7, 1.9)		This study
Mean		1.8	−1.1	−3	
		Southern Open Ocean			
367	~4 km	−1.3(−2, −0.8)[b]	−1.4(−2.3, 0.1)[b]	−0.1	*Kuypers et al.* [2004]
		Southern Coast			
Demerara rise					
1258		−0.8(−1.9, −0.2)	−1.8(−2.2, −0.3)		*Higgins et al.* [2012]
1260	~1 km	−1(−1.6, −0.5)	−2(−3, −0.3)		*Junium and Arthur* [2007]
1261	~1 km	n.a.	−2(−2.8, −0.3)		*Junium and Arthur* [2007]
Mean		−0.9	−1.9	−1	
		North Coast			
Bass River (new)	<30 m	1.4 (1.2,1.7)	1.3 (−0.2, 2)	−0.1	This study
		North-Eastern Coast			
Wunstorf	~100 m	n.a.	1 (−0.9,l)[b]		*Blumenberg and Wiese* [2012]
Wunstorf (new)		1.4 (0.6,2.6)	0.8 (−1.5, 3.3)		This study
Mean		1.4	0.9	−0.5	

[a]The mean $\delta^{15}N_{TN}$ before and during OAE 2 is presented, as well as the maximum and minimum values for each time interval. Standard deviations are shown as error bars in Figure 6; n.a. = not available.

[b]Evidence from biomarkers indicating a relatively high abundance of N_2 fixing cyanobacteria are indicated where available/present.

The exceptionally light $\delta^{15}N$ values during the event have been interpreted as indicators of high rates of N_2 fixation (Table 1) [*Kuypers et al.*, 2004; *Junium and Arthur*, 2007] and NH_4^+ upwelling [*Junium and Arthur*, 2007; *Higgins et al.*, 2012]. A dominant role for long-term diagenesis is generally discounted because of similar trends in compound-specific and bulk $\delta^{15}N$ records [*Robinson et al.*, 2012; *Junium et al.*, 2014]. At many sites, such as at Demerara Rise, in the southern part of the basin, the decline in $\delta^{15}N$ coincides with the rise in the stable carbon isotopic composition ($\delta^{13}C$) of sedimentary carbonate ($\delta^{13}C_{carb}$) and organic matter ($\delta^{13}C_{org}$) which is characteristic for OAE 2 [e.g., *Kuypers et al.*, 2002; *Tsikos et al.*, 2004]. The increase in N_2 fixation is assumed to be due to enhanced denitrification and an increase in P recycling linked to the expansion of low-oxygen conditions during the event [*Kuypers et al.*, 2002]. The widespread N_2 fixation during OAE 2 is supported by recent model studies of the biogeochemistry in the proto-North Atlantic [*Monteiro et al.*, 2012; *Ruvalcaba Baroni et al.*, 2014b].

Surprisingly, however, several studies of OAE 2 sediments report a parallel rise in $\delta^{15}N$ and $\delta^{13}C$ during the event [*Jenkyns et al.*, 2007] or the lack of a clear trend, whereas others have shown that such a trend exists (e.g., site 367; *Rau et al.* [1987] versus *Kuypers et al.* [2004]). Such deviations from the expected trend are only observed for sediments that have been subjected to a treatment with strong acid to remove carbonates prior to the $\delta^{15}N$ measurement. Acid treatment [*Lohse et al.*, 2000; *Brodie et al.*, 2011], in particular when followed by removal of the supernatant, is known to lead to removal of N compounds [*Nieuwenhuize et al.*, 1994]. As a consequence, changes in the $\delta^{15}N$ of sediments may no longer reflect changes in N dynamics in the proto-North Atlantic.

In this study, we compiled all the available $\delta^{15}N$ data in the proto-North Atlantic for coastal and deep-sea sediments from OAE 2 that were either treated with weak acid or not exposed to acid at all. Since little is known about the N dynamics in the open ocean and along the Northern Coast of the proto-North Atlantic, we expand the existing data set with new data for three open ocean sites and two coastal sites. Finally, we use

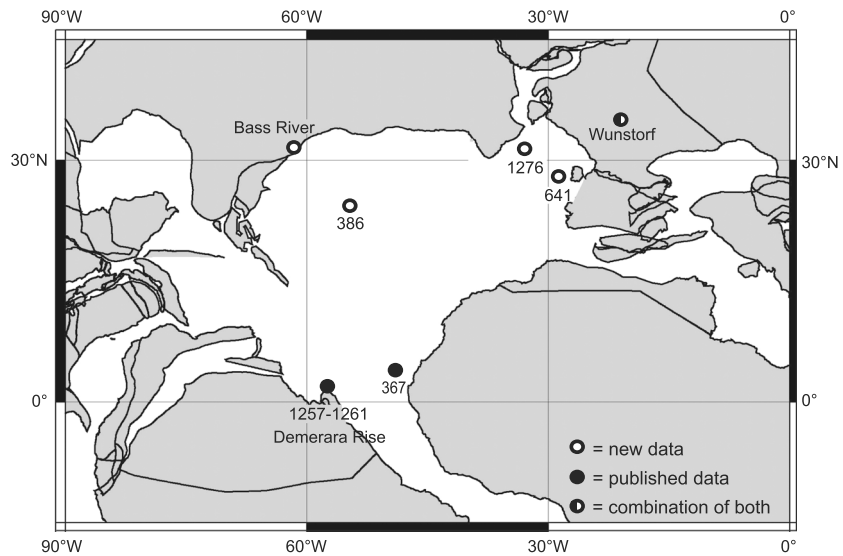

Figure 1. Paleogeographic map of the proto-North Atlantic during OAE 2, indicating the location of the sites where δ^{15}N data for samples that were not pretreated with acid are available for the Cenomanian-Turonian period. Open circles indicate the sites for which new $\delta^{15}N_{TN}$ data are presented in this study: Bass River, 1276, 641, and 386. Black circles are sites for which data of $\delta^{15}N_{TN}$ were published previously: 367 [*Kuypers et al.*, 2004] and 1258, and 1260 and 1261 [*Higgins et al.*, 2012; *Junium and Arthur*, 2007]. Black and white circles indicate the sites where both $\delta^{15}N_{TN}$ data were previously published [Wunstorf; *Blumenberg and Wiese*, 2012] and where new $\delta^{15}N_{TN}$ data with a higher resolution are presented. The map was generated at http://www.odsn.de/odsn/ services/paleomap/paleomap.html.

a box model for the proto-North Atlantic to assess whether the observed δ^{15}N values in the various coastal and open ocean settings can be explained by enhanced N_2 fixation and/or incomplete use of NH_4^+. While the overall proto-North Atlantic was low in dissolved oxygen, clear regional trends in its distribution can be distinguished, based on geological records [e.g., *Owens et al.*, 2012; *Ruvalcaba Baroni et al.*, 2014a]. As the N cycle is strongly affected by changes in dissolved oxygen, regional differences in sediment N isotope values in the proto-North Atlantic are expected.

2. Study Sites

All published isotope ratios of total sediment N ($\delta^{15}N_{TN}$) for nonacidified or weakly acidified samples from the proto-North Atlantic were compiled (Figure 1 and Table 1). This data compilation comprises four sites in the south (367 and 1258–1261 at Demerara Rise) [*Kuypers et al.*, 2004; *Junium and Arthur*, 2007; *Higgins et al.*, 2012] and one site in the north (Wunstorf) [*Blumenberg and Wiese*, 2012]. Sediments from five additional sites were selected for analysis in areas in the proto-North Atlantic for which there is either limited data or where previous records have a low depth resolution. These sites are located in the Northern Coast (Wunstorf and Bass River) and distributed over the Central Open Ocean (386, 641, and 1276).

2.1. Wunstorf: Northwest Germany

The Wunstorf core was drilled ~25 km west of Hannover, Germany (52°24.187′N, 09°29.398′E) [*Voigt et al.*, 2008]. During the Late Cretaceous the Hannover region was part of the epicontinental shelf sea that formed when large parts of Eurasia were flooded during the global Cenomanian transgression. The upper Cenomanian sediments, belonging to the Brochterbeck Formation (71.5–49.6 m below surface; mbsf), generally consist of white limestones and light grey marly limestones. The Brochterbeck Formation is overlain by the Hesseltal Formation (49.6–23.1 mbsf), which comprises the ~13.5 m thick OAE 2 interval. The Hesseltal Formation consists of rhythmically alternating multicolored marls, light grey (marly) limestones and black shales, with a maximum TOC content of ~3% [*Hetzel et al.*, 2011]. The retrieved sediments are estimated to have been deposited in water depths of 100 to 150 m [*Wilmsen*, 2003]. The OAE 2 interval was primarily identified based on detailed biostratigraphy, consistent with the English Chalk [*Voigt et al.*, 2008, and references therein]. The positive excursion in both $\delta^{13}C_{carb}$ (~2‰) [*Voigt et al.*, 2008] and $\delta^{13}C_{org}$ (~2.5‰) [*Du Vivier et al.*, 2014] at Wunstorf lags the positive excursion observed in other northeastern sites (e.g., Eastbourne)

[*Tsikos et al.*, 2004]. This alteration in the isotope curves at Wunstorf is probably a regional phenomenon which may be related to the lithology or diagenesis [*Voigt et al.*, 2008].

2.2. Bass River: New Jersey Shelf

The Bass River core was drilled as part of the New Jersey Coastal Plain, Ocean Drilling Program (ODP) Leg 174AX, New Jersey, USA (39°36′42N, 74°26′12W). The retrieved upper Cenomanian to lower Turonian sediments consist of homogenous dark gray, (micro)fossil-rich, micaceous silty clays to clayey silts, with a relatively low average total organic carbon content (TOC) of ~1% and a maximum of ~2.5% [*Bowman and Bralower*, 2005]. The persistent presence of benthic foraminifera and relatively modest TOC to total P ratios (TOC/P_{TOT}) indicate that bottom waters were never completely depleted in oxygen [*van Helmond et al.*, 2014a]. Assemblages of benthic foraminifera indicate that the entire sequence was deposited on a shallow shelf, predominantly in an inner neritic setting (water depth <30 m) [*Sugarman et al.*, 1999]. The approximately 13 m long OAE 2 interval was identified based on nannofossil biostratigraphy and ~2.5 ‰ positive shifts in $\delta^{13}C_{carb}$ and $\delta^{13}C_{org}$ [*Bowman and Bralower*, 2005; *van Helmond et al.*, 2014a].

2.3. Site 386: Central Bermuda Rise

Site 386 was drilled on the Central Bermuda Rise by Deep Sea Drilling Project (DSDP) Leg 43, some kilometers south-southeast of Bermuda (31°11.21′N, 64°14.94′W, 4793 m water depth). Site 386 is the most centrally located North Atlantic site yielding upper Cenomanian to lower Turonian sediments. The Late Cretaceous sediments predominantly consist of green, grey and black clay, and mudstones, with a maximum TOC content up to 13% [*van Helmond et al.*, 2014b], that were deposited at a water depth >2000 m. The OAE 2 interval was clearly identified by a ~2.5‰ positive shift in $\delta^{13}C_{org}$ [*van Helmond et al.*, 2014b].

2.4. Site 641: Galicia Bank

Site 641 was drilled during ODP Leg 103 and is located on the western margin of the Galicia Bank, offshore northwestern Spain (42°09.3′N, 12°10.9′W, 4646 m water depth). The upper Cenomanian to lower Turonian sediments generally consist of green and grey claystones, deposited at an estimated water depth of ~3500 m. The sequence may contain significant hiatuses. The OAE 2 interval itself is represented by a ~0.3 m of dark green and black shales, which is marked by a ~2.5‰ positive shift in $\delta^{13}C_{org}$ and an average TOC content of ~9%. The organic carbon background values are typically <0.1% [*van Helmond et al.*, 2014b].

2.5. Site 1276: Newfoundland Basin

Site 1276 was drilled during ODP Leg 210, in the Newfoundland Basin, offshore the eastern Canadian continental margin (45°24.3198′N, 44°47.1496′W, 4565 m water depth). The mid-Cretaceous sequence consists of mud-dominated gravity flow deposits. The OAE 2 interval itself, however, consists of a 3.5 m thick stack of mainly pelagic sediments [*Urquhart et al.*, 2007], supported by a drastic drop of terrestrial palynomorphs, with an average TOC content of 4% and maximum values up to 13% [*Sinninghe Damsté et al.*, 2010]. Large positive shifts of ~4.5‰ in $\delta^{13}C_{org}$ and >5‰ in the stable carbon isotopes of the bacterial biomarker, C_{31} 17β, 21β(H)−hopane, define the OAE 2 interval [*Sinninghe Damsté et al.*, 2010].

3. Material and Methods

3.1. Sediment Geochemistry

The Bass River core was sampled at and by the Rutgers Core Repository (Rutgers University, New Jersey, USA). The Wunstorf, 386, 641, and 1276 cores were sampled at the International Ocean Discovery Program (IODP) core repository in Bremen (Marum, Bremen University, Germany). After shipment to Utrecht, aliquots of the samples were cleaned, ground, freeze-dried, and subsequently stored cool and dry until analysis. All five cores contain sediments of the Cenomanian-Turonian transition.

Total sediment N (N wt %) and $\delta^{15}N_{TN}$ were measured using a Fisons Instruments CNS NA 1500 analyzer coupled to a Thermo Delta Plus isotope ratio spectrometer. The average analytical uncertainty based on analyses of duplicate sediment samples was 0.0041 wt % ($1\sigma = 0.0043$) for N and 0.173‰ ($1\sigma = 0.177$) for $\delta^{15}N_{TN}$.

3.2. Model

The model used in this study is a simplified version of the multibox model of *Ruvalcaba Baroni et al.* [2014a, 2014b] that describes the coupled dynamics of particulate organic carbon, particulate organic and dissolved N, P, and oxygen in the proto-North Atlantic during OAE 2. Here we use the same settings for all cycles as those in their multibox model (MB1), but we exclude regions for which data of $\delta^{15}N_{TN}$ are not available (e.g., Western Interior Seaway). On the basis of results of MB1, *Ruvalcaba Baroni et al.* [2014b] suggest that N_2

Table 2. Relevant Rates and Components Affecting the δ^{15}N in the MB2 Model for Pre-OAE 2 and OAE 2 Conditions[a]

	Central Open Ocean		Northern		Northeastern		Southern		Tethys Gateway	
	Pre-OAE 2	OAE 2	Pre-OAE 2	OAE 2	Pre-OAE 2	OAE 2	Pre-OAE 2	OAE 2	Pre-OAE 2	OAE 2
NH_4^+UP	0	0.02	0	1.1	0	0	0	3.9	0	0.5
NO_3^-UP	2	2.4	6.8	1.3	0.2	0.4	4.8	1.2	1.1	0.7
NH_4^+LT	0	2.8	0	0.7	0	0.1	0	0.3	-	-
NO_3^-LT	5.1	2.1	2	1.5	0.2	0.9	0.2	0.4	-	-
TOTNin	7.1	7.32	8.8	4.6	0.4	1.4	5	5.8	1.1	1.2
N2FIX	0.25	5.2	0.3	1.5	0.1	0.3	3	1.5	0.04	1.2
DENW	1.2	9.7	0	0.3	0	0.04	0.1	0.1	0	0.03
DENS	0.84	1.5	0.2	1.1	0	0.06	2	0	0.02	0.1
DEN_{TOT}	2.04	11.5	0.2	1.4	0	0.1	2.1	0.1	0.02	0.14
NIT	3.18	0	2	0	0.5	2.7	3.2	0	0.5	0
$[NH_4^+]_{sub}$	0	29	0	11	0	0	0	31	0	9
$[NO_x^-]_{sub}$	44	0	26	12	16	14	35	10	16	7
$[O_2]_{sub}$	144	11	116	11	157	94	30	0	140	27

[a]Major processes in the N cycle (Tmol N y^{-1}) and concentrations (μM) of subsurface ammonium ($[NH_4^+]_{sub}$), nitrate ($[NO_x^-]_{sub}$), and oxygen ($[O_2]_{sub}$) in the Central Open Ocean and in coastal regions are listed. The abbreviations NH_4^+LT, NH_4^+UP, and DEN_{TOT} refer to the upwelling flux of recycled NH_4^+, lateral transport of NH_4^+, and the sum of water column (DENW) and sedimentary denitrification (DENS) for each region. NO_3^-LT, NO_3^-UP, and TOTNin refer to the upwelling flux of NO_3^-, lateral transport of NO_3^-, and total input of N to surface waters. N_2 fixation and nitrification are referred to as N2FIX and NIT.

fixation was widespread during OAE 2. Uptake of NH_4^+ by primary producers is suggested to be important in all upwelling areas. Denitrification is significant in the Central Open Ocean and along the Northern Coast. All rates of N processes in our simplified model (MB2) are summarized in Table 2.

3.2.1. Model Structure

We use the MB2 model to assess whether we can explain the δ^{15}N values for sediments in the Central Open Ocean and four coastal regions during OAE 2. The Central Open Ocean box includes sites 386, 603, and 1276. The coastal boxes are the Southern Coast (upwelling region where Demerara Rise is located), the Northern Coast (upwelling region where Bass River is located), and the North-Eastern Coast (downwelling region where Wunstorf is located). The Tethys Gateway is also included in the MB2 model because lateral exchange from the gateway into the Central Open Ocean is important in the multibox model. Further details on the segmentation and water fluxes of the model are presented in Text S1 in the supporting information.

The N pools included in the model are NO_x^-, NH_4^+, and PON. In surface waters, only one combined inorganic nitrogen (DIN) reservoir is considered (note that surface NH_4^+ is initially close to zero). A full description of the model can be found in *Ruvalcaba Baroni et al.* [2014a] and in *Ruvalcaba Baroni et al.* [2014b]. Relevant parametrizations and rate laws for N processes are summarized in Tables 3 and 4. Perturbations in the MB2 model to simulate OAE 2 conditions are taken from the baseline OAE 2 scenario in *Ruvalcaba Baroni et al.* [2014b] (their BsLi-N).

3.2.2. Nitrogen Isotope Dynamics

The MB2 model resolves the dynamics of the two stable N isotopes, ^{15}N and ^{14}N. The conventional δ notation (‰) for N isotope ratios with respect to atmospheric N (R_{atm}) is

$$\delta^{15}N_{res} = \left(\frac{R_{Nres}}{R_{atm}} - 1\right) \cdot 1000, \tag{1}$$

where R_{Nres} is the ratio between $^{15}N_{res}$ and $^{14}N_{res}$ of the corresponding N reservoir (N_{res}) in the ocean. We explicitly model the reservoir for $^{15}N_{res}$, and we calculate $^{14}N_{res}$ from the total N pool ($^{14}N_{res} = TOTN_{res} - {}^{15}N_{res}$) to detect changes in $\delta^{15}N_{res}$ with time. The ^{15}N pools included in the model are for DIN, NO_x^-, NH_4^+, and PON.

In our initial conditions, $^{15}N_{res}$ in the ocean accounts for the same percentage as in the atmosphere (0.366% of the total atmospheric N):

$$^{15}N_{res} = TOTN_{res} \cdot 0.00366; \tag{2}$$

Table 3. Relevant Parametrizations for the Processes Related To the N Cycle[b]

N Process	Parametrization
Primary productivity	$PP = kphoto \cdot Red_{C:P} \cdot W \cdot \min\left(\frac{[NO_x^-]}{16} \cdot \frac{[NO_x^-]}{[NO_x^-]+K_N}, [SRP] \cdot \frac{[SRP]}{[SRP]+K_P}\right)$
NO_x^- uptake	$NUPTAKE = Red_{N:C} \cdot PP$
NH_4^+ uptake	
Surface N_2 fixation	$NFIX_s = knf_s \cdot W \cdot 16 \cdot [SRP] \cdot \frac{[SRP]}{[SRP]_o} \cdot \left(\frac{K_{NF}}{[NO_x^-]+K_{NF}}\right)^{nfNs}$
Subsurface N_2 fixation	$NFIX_{sub} = knf_{sub} \cdot W \cdot 16 \cdot ([SRP] \cdot \frac{[SRP]}{[SRP]_o})^{nfP} \cdot \left(\frac{K_{NF}}{[NO_x^-]+[NH_4^+]+K_{NF}}\right)^{nfNb}$
Nitrification	$NITRI = knox \cdot [NH_4] \cdot W \cdot \frac{[O_2]}{[O_2]+K_{O2}}$
Water column	$DENW = \sqrt{kdenw \cdot [NO_x^-] \cdot W} \cdot \frac{[NO_x^-]}{[NO_x^-]+K_{NO}} \cdot \left(\frac{K_{O2}}{[O_2]+K_{O2}}\right)^{dnfO}$
Denitrification	
Sediment	$DENS = \sqrt{kdens \cdot [NO_x^-] \cdot W} \cdot \frac{[NO_x^-]}{[NO_x^-]+K_{NO}} \cdot \frac{K_{O2}}{[O_2]+K_{O2}}$
Denitrification	

[a]Here *kphoto*, *knf*, *knox*, *kdenw*, and *kdens* are rate constants; Red is the Redfield ratio between C:N:P (106:16:1); and K_N, K_P, K_{NF}, K_{O2}, and K_{NO} are the half-saturation constants relative to each process. *W* refers to the size of the water box in cubic meter; [SRP] is the concentration of the soluble reactive phosphorus in mol per liter; and *nf*N*s*, *nfNb*, *nfP*, and *dnfO* are moderator factors. For more details, see *Ruvalcaba Baroni et al.* [2014b].

hence, $\delta^{15}N_{res}^{initial} = 0$. After reaching a geochemical steady state for N pools during pre-OAE 2, fractionation factors for all N processes are included (Table 4), with the exception of N uptake (initially zero). The model is then run until a new isotopic equilibrium state is reached before implementing OAE 2 perturbations.

The distribution of components with time are calculated using the set of differential equations shown in Text S2 and Table S1 in the supporting information. The equations for each individual ^{15}N process are summarized in Table 4.

Reported values of enrichment factors (ϵ) for key N processes differ widely, especially regarding denitrification in sediments and the water column, uptake of NH_4^+, and nitrification. In general, we chose the most commonly used and/or most recently suggested ϵ for each process, except for N_2 fixation and N uptake (details in section 3.2.3). N_2 fixation has a small fractionation effect, producing cells with $\delta^{15}N$ values that are relatively close or slightly depleted (generally −1 but up to −3‰) relative to atmospheric values [e.g., *Capone et al.*, 1997; *Brandes and Devol*, 2002]. In order to assess whether the isotopic signal of N could be explained by N_2 fixation alone, we chose the most negative ϵ reported in literature for the most common N_2 fixers. *Kritee et al.* [2012] reported a range of ϵ values (−25 to −5‰) for denitrification based on culture experiments, but they also suggested that an ϵ close to −10‰ is more representative for water column denitrification in oceanic environments. We have therefore adopted an ϵ of −10‰ in our model simulations. The compilation of the reported ϵ as well as the chosen values for this study are listed in Table 4. A simplified N isotope cycle as implemented in our model is shown in Figure S1. Details about the response of water column $\delta^{15}N$ values are available in Text S2 (Table S2 and Figure S2) in the supporting information.

As records of $\delta^{15}N_{TN}$ mainly represent the isotopic composition of organic matter, comparison between model results and data is only possible for the $\delta^{15}N$ of PON. Because we aim to capture the major shift in $\delta^{15}N_{TN}$ for each region during the Cenomanian-Turonian transition, we average the $\delta^{15}N_{TN}$ values measured for pre-OAE 2 and OAE 2 intervals, respectively. Additionally, we calculate the standard deviation of each averaged $\delta^{15}N_{TN}$ and identify the full range for both time intervals. In the case where several $\delta^{15}N_{TN}$, records are available for one single region, and data matched our stringent quality criteria (i.e., no strong acidification; Table 1), all $\delta^{15}N_{TN}$ values for that region are included in the average. In order to differentiate the $\delta^{15}N$ from records and from the model, we refer to the modeled isotopic composition of the organic N as $\delta^{15}N_{model}$.

3.2.3. Sensitivity Analysis and Numerical Experiments

Because the effect of N_2 fixation and partial NH_4^+ uptake by phytoplankton on the isotopic fractionation of N is uncertain, we perform a sensitivity analysis for both these processes. We first consider an ϵ for N_2 fixation of −3‰ (Table 4) and combine it with a large range of ϵ values for partial NH_4^+ uptake (−4 to −16‰). Although some laboratory studies reported stronger fractionations with ϵ values down to −27‰ [*Hoch et al.*, 1992;

Table 4. Rate Equations for the ^{15}N Processes, the Corresponding Range of Enrichment Factors (ϵ in ‰) Found in the Literature and the Values Used in the Model[a]

N Process	^{15}N Equation	ϵ Range	ϵ in Model
NO_x^- uptake	$NUPTAKE15 = \alpha_{PP} \cdot R_{NOx} \cdot NUPTAKE$	−5 to 0[c]	0[b]
NH_4^+ uptake		−27 to −4[d,e]	−4[b]
N_2 fixation	$N2FIX15 = \alpha_{N2FIX} \cdot R_{atm} \cdot N2FIX$	−3 to 0[f,l,m]	−3[b]
N release	$NREM15 = \alpha_{NREM} \cdot R_{PON} \cdot NREM$	0	0
PON export	$NEXP15 = \alpha_{EX} \cdot R_{PON} \cdot NEXP$	−1 to 0[h]	−1
Ammonification	$AMMONI15 = \alpha_{AMMONI} \cdot R_{PON} \cdot AMMONI$	0	0
Nitrification	$NIT15 = \alpha_{NIT} \cdot R_{NH4} \cdot NIT$	−35 to −7[i,j]	−20
Water column Denitrification	$DENW15 = \alpha_{DENW} \cdot R_{NOx} \cdot DENW$	−25 to −5[g,k]	−10
Sediment Denitrification	$DENS15 = \alpha_{DENS} \cdot R_{NOx} \cdot DENS$	−6 to −1[f,k,l]	−4
PON burial	$NBUR15 = \alpha_{BURN} \cdot R_{PON} \cdot NBUR$	−6 to 0[i]	0
Transport of inorganic N	$N15T = R_{source} \cdot NT$	none	none

[a]The fractionation factor is calculated as $\alpha = \frac{\epsilon}{1000} + 1$ for each corresponding process (in subscripts). R is the $\frac{^{15}N}{^{14}N}$ ratio of the corresponding source pool indicated with subscripts.
[b]For a full description of ϵ values of NO_x^- uptake and NH_4^+ uptake see sections 3.2.2 and 3.2.3.
[c]*Waser et al.* [1998].
[d]*Altabet and Francois* [1994].
[e]*Hoch et al.* [1994].
[f]*Brandes and Devol* [2002].
[g]*Granger et al.* [2008].
[h]*Higgins et al.* [2011].
[i]*Brandes and Devol* [1997].
[j]*Mariotti et al.* [1981].
[k]*Kritee et al.* [2012].
[l]*Carpenter et al.* [1997].
[m]*Capone et al.* [1997].

Waser et al., 1998], field observations usually show less fractions; we therefore limited our sensitivity analysis to an ϵ down to −16‰. We then perform a sensitivity test for N_2 fixation, where ϵ goes from 0 to −7‰ [*Zhang et al.*, 2014] and an ϵ for NH_4^+ uptake of −4‰. In addition, the choice of our fractionation factor for water column denitrification may affect the results of the former sensitivity analysis. Therefore, we also tested the response of our model to changes in the fractionation factor for denitrification.

We also perform three main numerical experiments (E1, E2, and E3) with the MB2 model in order to identify which processes in the N cycle could potentially contribute to the $\delta^{15}N_{TN}$ observed in OAE 2 sediments. Denitrification and nitrification, when unbalanced, may influence the $\delta^{15}N$ of the water column [*Ryabenko*, 2013] and thus the signal of the buried organic N. We build an additional model (MB3) with all the same characteristics as the MB2 model but with new parametrizations of nitrification and water column denitrification (Text S3). The new parametrization in MB3 reduces water column denitrification and increases nitrification without the need to alter the initial conditions. We then repeat the three experiments with the MB3 model in order to assess the effect of reduced denitrification on $\delta^{15}N_{TN}$. The experiments performed with the MB2 model are denoted with subscript $_{MB2}$ and those carried out with the MB3 model with subscript $_{MB3}$.

We start with a simple experiment (E1) assuming complete N assimilation by phytoplankton. Therefore, primary production has no fractionation (α_{PP}=1). For experiment 2 (E2), we assess the fractionation effect of primary production due to incomplete uptake of N in surface waters. We assume that the upwelled NH_4^+ is neither fully consumed nor fully oxidized in surface waters due to excess NH_4^+. Because N uptake in the surface layer is modeled as one single pool, α_{PP} accounts for the contribution of all inorganic N, including NH_4^+, and their isotope effect. Moreover, α_{PP} is adjusted for each region according to the amount of upwelled NH_4^+ relative to the total upwelled N. The fractionation factor is then calculated as

$$\alpha_{PP} = \left(P_{NH_4^+} \cdot \epsilon_{PP_{NH}} + P_{NO_x^-} \cdot \epsilon_{PP_{NO}}\right)/1000 + 1, \quad (3)$$

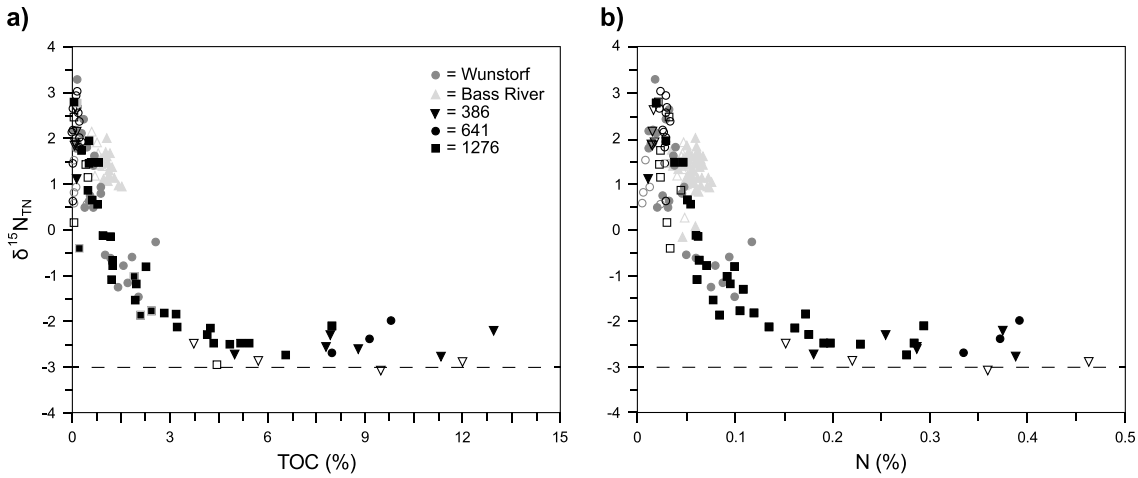

Figure 2. (a) Total organic carbon (TOC) and (b) total N (N) versus $\delta^{15}N_{TN}$. Coastal sites are indicated in light gray. Open and closed symbols indicate pre-OAE 2 and OAE 2 sediments, respectively. The lower limit of $\delta^{15}N_{TN}$ is indicated with the dashed horizontal line. Sediment N, $\delta^{15}N_{TN}$ and TOC values for each site are given in Tables S5–S9 in the supporting information.

where $P_{NH_4^+}$ and $P_{NO_x^-}$ are the portion of upwelled NH_4^+ and NO_x^- relative to total upwelled N, respectively (e.g., $P_{NH_4^+} = \frac{NH_4^+UP}{TOTNUP}$, where NH_4^+UP and TOTNUP represent upwelling of NH_4^+ and total dissolved N, respectively). Because NH_4^+ dominates the system in anoxic conditions, we assume no fractionation effect for NO_x^- uptake ($\epsilon_{PP_{NO}}$ = 0‰). When NH_4^+ replaces NO_x^-, the effect of incomplete NH_4^+ uptake may become important [*Hoch et al.*, 1992, 1994]. The enrichment factor for NH_4^+ ($\epsilon_{PP_{NH}}$) in our model is then nonzero and is chosen from our sensitivity analysis. In Table 2, we show the upwelling fluxes for NH_4^+ and NO_x^- given by the model in each region. In E2, α_{PP} values in the Central Open Ocean and the North-Eastern Coast are assumed to be 1, because the quantity of upwelled NH_4^+ is very small.

Lateral transport in the multibox model is important even in surface waters. All regions are influenced by the incoming waters of one or more neighboring areas. As a third experiment (E3), we consider the additional effect that lateral transport of NH_4^+ to surface waters can have on fractionation during primary production. We estimate the lateral transport of NH_4^+ and NO_x^- for each region and calculate α_{PP} following equation (3) but including both upward and lateral transport of N (full description in Text S4). A summary of calculated α_{PP} values for each experiment is given in Table S4.

4. Results

4.1. Relationship Between TOC, TOC/N, and $\delta^{15}N_{TN}$

A scatterplot of $\delta^{15}N_{TN}$ versus TOC for all five locations reveals a clear, nonlinear, negative relation between TOC and $\delta^{15}N_{TN}$ at both coastal and open ocean sites (Figure 2a). When the TOC content is low (<2%), $\delta^{15}N_{TN}$ decreases sharply with increasing TOC, with most $\delta^{15}N_{TN}$ being positive. With further increasing TOC, all $\delta^{15}N_{TN}$ values are negative until they become nearly constant with a distinct minimum of approximately −3‰(when TOC > 4%). A similar relation is observed between $\delta^{15}N_{TN}$ and total N (Figure 2b). A Keeling plot of OAE 2 $\delta^{15}N_{TN}$ revealed an end-member" value for N_2 fixation of ∼−3‰. Note that most $\delta^{15}N_{TN}$ at both coastal sites (Wunstorf and Bass River), together with most values for pre-OAE 2 conditions at the other sites, are positive.

4.2. Coastal Sites: Wunstorf and Bass River

The OAE 2 interval at Wunstorf and Bass River (Figure 3) is well demarcated by the positive excursion of $\delta^{13}C_{org}$ that includes the onset and the final recovery phase at both coastal sites [e.g., *Voigt et al.*, 2008; *van Helmond et al.*, 2014a]. Although more extreme at Wunstorf than at Bass River, all chemical profiles show large changes during OAE 2 relative to preexcursion values, with TOC, TOC/P_{TOT}, and N increasing and $\delta^{15}N_{TN}$ decreasing. In general, the Wunstorf site is characterized by higher TOC (∼3%), TOC/P_{TOT} (∼125), and N (∼0.1%), as well as lower $\delta^{15}N_{TN}$ (∼−1‰) when compared to Bass River.

All chemical profiles for the two coastal sites show a higher variability during OAE 2 compared to pre-OAE 2 conditions. This is most pronounced at Wunstorf. While at Bass River, a negative $\delta^{15}N_{TN}$ (<0‰) occurs near

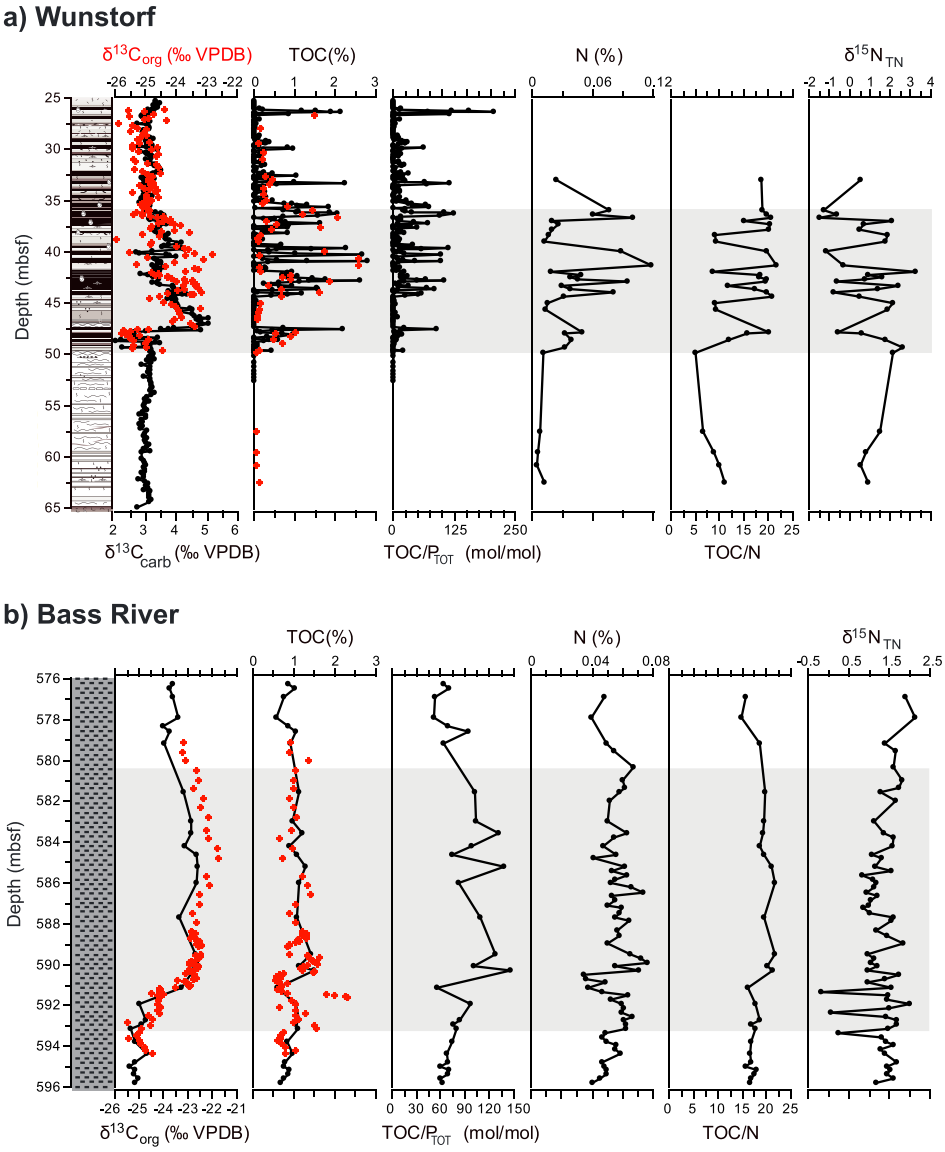

Figure 3. Geochemical results across Oceanic Anoxic Event 2 (OAE 2) at two coastal sites: (a) Wunstorf and (b) Bass River plotted against mbsf. (from left to right) $\delta^{13}C$, TOC content, total organic carbon to total phosphorus ratio (TOC/P_{TOT}), total nitrogen content (N), TOC/N ratios, and isotopic signal of total nitrogen ($\delta^{15}N_{TN}$) in bulk sediments. VPDB—-Vienna Peedee belemnite. $\delta^{13}C_{org}$ values in Figure 3a are from *Voigt et al.* [2008] (black) and *Du Vivier et al.* [2014] (red). Measurements of TOC and TOC/P_{TOT} are from *Hetzel et al.* [2011] (black). TOC measurements (red) are from *van Helmond et al.* [2015]. Stratigraphy is from *Voigt et al.* [2008]. In Figure 3b $\delta^{13}C_{org}$ and TOC values are from *van Helmond et al.* [2014a] (black) and *Bowman and Bralower* [2005] (red). At Bass River and Wunstorf, TOC/P_{TOT} are from *van Helmond et al.* [2014a] and newly calculated for this study, respectively. New measurements for both sites are for N and $\delta^{15}N_{TN}$.

the onset of OAE 2; at Wunstorf, large negative shifts in $\delta^{15}N_{TN}$ are observed throughout the entire OAE 2 interval. During OAE 2, $\delta^{15}N_{TN}$ ranges from −1.5 to +3‰ and from −0.5 to +1.5‰ at Wunstorf and Bass River, respectively. In both $\delta^{15}N_{TN}$ profiles, all major negative shifts are related to maxima in $\delta^{13}C_{org}$, TOC, TOC/P_{TOT}, and N. While TOC/N ratios mirror the $\delta^{15}N_{TN}$ signal at Wunstorf, at Bass River they are fairly constant throughout the OAE 2 interval (~20).

4.3. Central Open Ocean: Sites 386, 641, and 1276

During the OAE 2 interval, identified by the positive excursion of $\delta^{13}C_{org}$, a large increase in TOC, TOC/P_{TOT}, TOC/N, and N content occurs at all three open ocean sites (Figure 4). Contents of TOC are highest at sites 386 and 1276 (~13%).

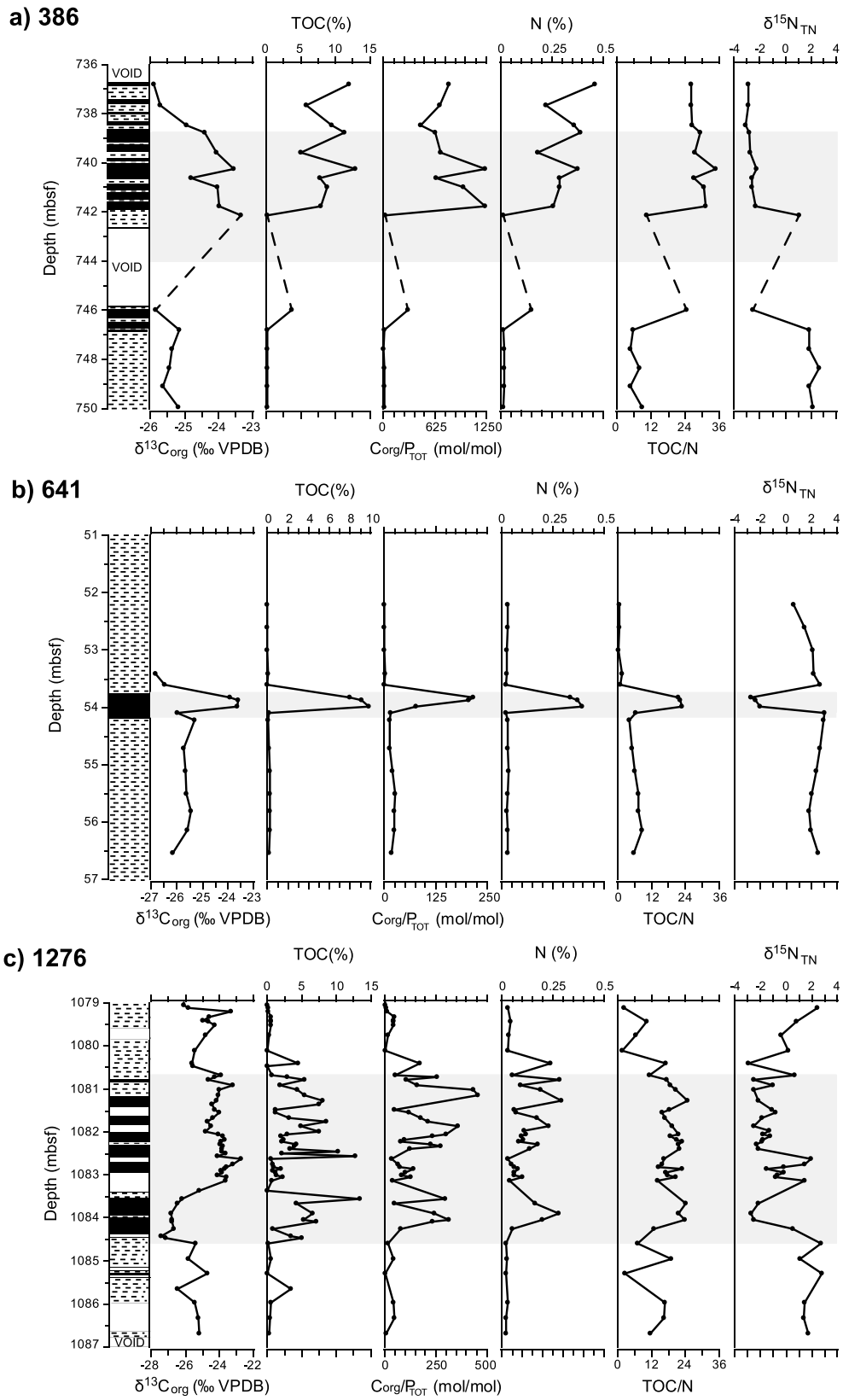

Figure 4. Geochemical results across Oceanic Anoxic Event 2 (OAE 2) at (a) 386 and (b) 641 and (c) 1276 plotted against mbsf. (from left to right) $\delta^{13}C_{org}$ and TOC content, TOC/P_{TOT}, N, TOC/N ratios, and $\delta^{15}N_{TN}$. Abbreviations as in Figure 3. Supporting information are from *van Helmond et al.* [2014b] and *Sinninghe Damsté et al.* [2010].

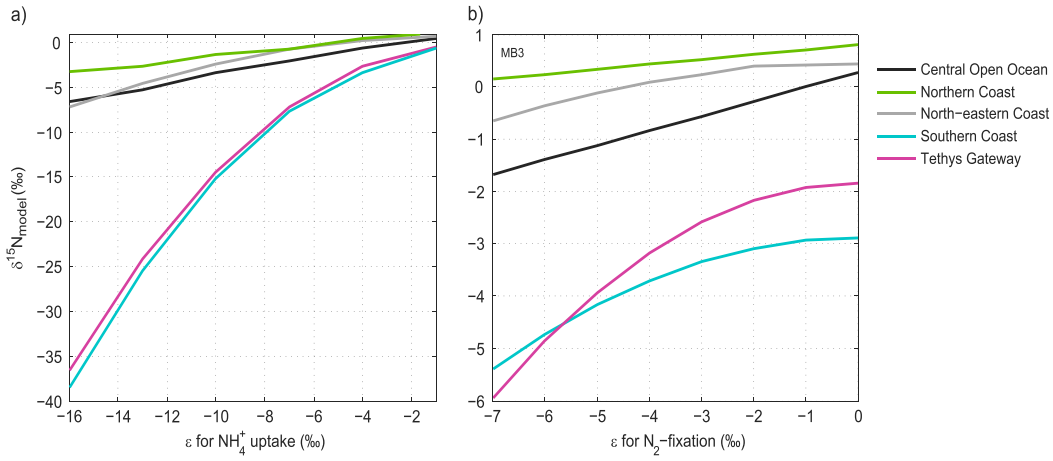

Figure 5. Sensitivity analysis of (a) partial NH_4^+ uptake by phytoplankton and (b) N_2 fixation to the fractionation factor. Range of ϵ follow values from literature.

At site 386 (Figure 4a), the actual initiation of OAE 2 was not recorded. At the first point within OAE 2, TOC, TOC/P_{TOT}, and N are near background values. From then onward, $\delta^{15}N_{TN}$ mirrors the TOC and N data until the termination where there is a decoupling between TOC, TOC/P_{TOT}, N, and $\delta^{15}N_{TN}$. Nonetheless, TOC, TOC/P_{TOT}, and N remain high, and $\delta^{15}N_{TN}$ is fairly constant around −3‰. The $\delta^{15}N_{TN}$ during OAE 2 at this location ranges from ∼−3 to +2‰, while the absolute shift from pre-OAE 2 to OAE 2 conditions is ∼−5.5‰.

At site 641 (Figure 4b), the $\delta^{15}N_{TN}$ profile presents a sharp decrease at the onset and a relatively fast recovery toward the termination of OAE 2. In this case, the most negative value $\delta^{15}N_{TN}$ (−3‰) coincides with the highest TOC/P_{TOT} (∼240). The largest absolute $\delta^{15}N_{TN}$ shift from pre-OAE to OAE 2 of all three sites, is observed at this site (∼−6‰).

At site 1276 (Figure 4c), all profiles show a high variability with several maxima and minima throughout the OAE 2 interval. Most peaks in $\delta^{15}N_{TN}$ coincide with lows in TOC, TOC/P_{TOT}, and N. While TOC/P_{TOT} increase significantly at the onset of OAE 2, the highest value (∼457) occurs toward the termination of OAE 2. The lower $\delta^{15}N_{TN}$ values are close to ∼−3‰, as observed at sites 386 and 641. The absolute shift from pre-OAE 2 to OAE 2 in $\delta^{15}N_{TN}$ is similar to that at site 386 (∼−5.5‰).

4.4. Model Results

The sensitivity analysis for both partial NH_4^+ uptake and N_2 fixation shows a nonlinear relationship with respect to ϵ (Figure 5). These processes respond similarly to changes in ϵ for every region, when ϵ falls between −4 to −1 and −3 to 0‰ for NH_4^+ uptake and N_2 fixation, respectively. In this range, both of these processes are important in shaping the $\delta^{15}N_{model}$. Below an ϵ of −4‰, even with a relatively small ϵ for N_2 fixation, partial NH_4^+ uptake dominates the $\delta^{15}N_{model}$. Note that in our model, water column denitrification has a much smaller effect than partial NH_4^+ uptake and N_2 fixation (Text S2 and Figure S3). For the full ϵ range of water column denitrification, only an increase of approximately 0.5 ‰ occurs in the most sensitive region, the Southern Coast.

In the MB2 model, rates of N_2 fixation are higher than rates of upwelled NH_4^+ in all regions, except in the Southern Coast (Table 2). With the new set of equations described in Text S2, total denitrification rates (Table S1) are generally lower. This leads to an increase in NO_x^- concentrations in most regions, which lowers N_2 fixation but increases organic matter production. Consequently, NH_4^+ concentrations are significantly higher, despite high nitrification rates (Table S1), in the MB3 model than in the MB2 model. This is reflected in the generally more depleted $\delta^{15}N_{model}$. Nevertheless, sensitivity results of the MB2 model are very similar to those of MB3 (therefore, not shown), where below an ϵ of −4‰, partial NH_4^+ uptake dominates the isotopic signal.

In Figure 6, we show the results of $\delta^{15}N_{model}$ for all numerical experiments and compare them to the average $\delta^{15}N_{TN}$, as well as its standard deviation and the most extreme values for the pre-OAE 2 and OAE 2 intervals. With the exception of $E3_{MB3}$, results of the MB2 and MB3 model are very similar; therefore, $E1_{MB3}$ and $E2_{MB3}$ results are not shown. The $\delta^{15}N_{model}$ in all experiments besides $E3_{MB3}$ during OAE 2 are close to the mean

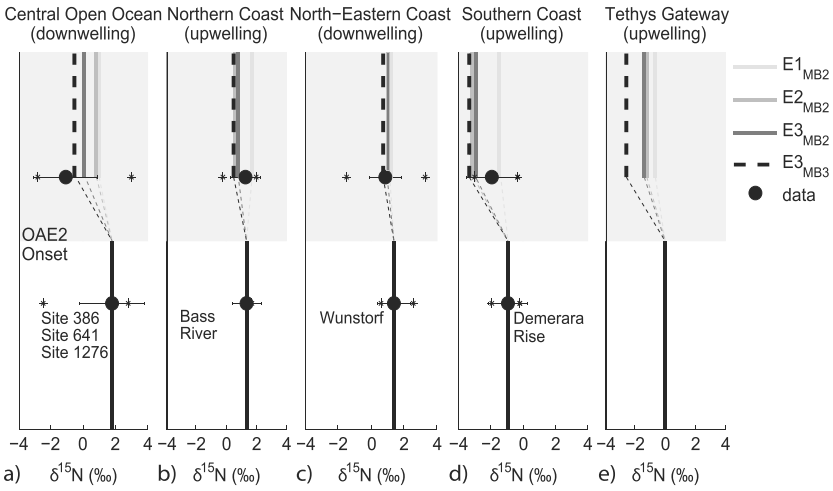

Figure 6. Model results (bold lines) for experiments 1–3, simulating the mean shift in δ^{15}N from pre-OAE 2 to OAE 2 (gray shade) in (a) the Central Open Ocean, (b) Northern Coast, (c) North-Eastern Coast, (d) Southern Coast and (e) Tethys Gateway. Experiments are the following: no fractionation due to primary productivity (E1), fractionation effect by primary productivity due to NH_4^+ input to surface waters from upwelling (E2), and fractionation effect by primary productivity due to NH_4^+ input to surface waters from upwelling and lateral transport (E3). E2 and E3 assume incomplete uptake of NH_4^+ by phytoplankton growth. Results performed with the MB2 and MB3 models are indicated with subscripts $_{MB2}$ and $_{MB3}$, respectively. Observations of the mean $\delta^{15}N_{TN}$ shift from pre-OAE to OAE 2 (black plain circles) together with the ± standard deviation (horizontal black lines) and the lowest and highest value during OAE 2 (stars) are plotted in each corresponding region for comparison. The $\delta^{15}N_{TN}$ of sites 386, 641, and 1276 are averaged in Figure 6a. $\delta^{15}N_{TN}$ values at Demerara Rise are taken from bulk sediment data of *Higgins et al.* [2012]. Note that the time considered for both pre-OAE 2 and OAE 2 is ~200 and ~500 kyr, respectively.

$\delta^{15}N_{TN}$ or within the ± standard deviation in most regions. Experiment $E3_{MB3}$ shows the most negative values, notably in areas dominated by downwelling (i.e., Central Open Ocean and North-Eastern Coast). In the Central Open Ocean, however, the full range in $\delta^{15}N_{model}$ is not captured (Figure 6a).

5. Discussion

5.1. Trends in $\delta^{15}N_{TN}$ During OAE 2: N_2 Fixation and NH_4^+ Uptake

Data of $\delta^{15}N_{TN}$ for OAE 2 matching our criteria are only available for a few sites (Table 1). At all these sites, similar trends are observed, with the perturbation due to OAE 2 being most pronounced in the Central Open Ocean (Figures 4 and 6). The magnitude of the absolute shift in $\delta^{15}N_{TN}$ per region is tightly linked to the redox conditions in the proto-North Atlantic. When considering mean values, the smallest absolute $\delta^{15}N_{TN}$ shift from pre-OAE 2 to OAE 2 occurred at Bass River and Wunstorf (~−0.1 and −0.5‰, respectively). As indicated by the TOC/P_{TOT} ratios, conditions along the north coast, in particular at Bass River [*van Helmond et al.*, 2014a], were not as reducing as in the open ocean [*van Bentum et al.*, 2012; *van Helmond et al.*, 2014b] and Southern Coast [e.g., *Sinninghe Damsté and Köster*, 1998; *Kuypers et al.*, 2002]. In the euxinic southern proto-North Atlantic (at Demerara Rise and at site 367), the absolute shift in $\delta^{15}N_{TN}$ is, however, smaller than in the Central Open Ocean. The small $\delta^{15}N_{TN}$ shift during the Cenomanian-Turonian transition can be explained by sporadic anoxia prior to but near the onset of OAE 2 in the south [e.g., *Sinninghe Damsté and Köster*, 1998; *Kuypers et al.*, 2002].

Our models (MB2 and MB3) aim to explain the mean absolute shifts in $\delta^{15}N_{TN}$ from pre-OAE 2 to OAE 2 conditions. In general, the MB2 model captures the mean $\delta^{15}N_{TN}$ values in all regions (Figure 6). In experiments $E1_{MB2}$ to $E3_{MB2}$, the largest shift occurs in the open ocean (Figure 6a) in agreement with observations of Table 1. In the MB2 model, N_2 fixation rates are high everywhere, being highest in the Central Open Ocean during OAE 2 (Table 2). This suggests that N_2 fixation was a major process controlling the $\delta^{15}N_{TN}$ signal throughout the entire OAE 2 event. This is in agreement with what was previously suggested [e.g., *Junium and Arthur*, 2007; *Kuypers et al.*, 2004; *Blumenberg and Wiese*, 2012], although each of these studies was based on sites from a single region. Our model results and data show that N_2 fixation was also significant in the Central Open Ocean.

The effect of early diagenesis on $\delta^{15}N_{TN}$ is expected to increase with water depth due to prolonged oxygen exposure of sediments in low sedimentation rate environments [e.g., *Möbius et al.*, 2010; *Robinson et al.*, 2012]. In the Central Open Ocean, the pristine $\delta^{15}N_{TN}$ signal in pre-OAE 2 conditions may have been lower than the one measured in our samples, leading to a smaller shift in $\delta^{15}N_{TN}$ from pre-OAE 2 to OAE 2 conditions. Because our model does not include diagenesis, the $\delta^{15}N_{model}$ in the Central Open Ocean only captures the N isotope signal of the intact deposited organic matter (Figure 6a).

Extreme values recorded in the $\delta^{15}N_{TN}$ profiles (Figure 4) are best captured by experiment $E3_{MB3}$ (performed with the MB3 model) in both the Central Open Ocean and coastal areas. In the MB3 model, accumulation of NH_4^+ in bottom waters is higher than in the MB2 model (Table S3), leading to a higher fractionation effect of primary production due to incomplete uptake of NH_4^+ in $E3_{MB3}$ when compared to $E3_{MB2}$. The more pronounced $\delta^{15}N_{TN}$ shifts in $E3_{MB3}$, which best matches the data, suggests that lateral transport of NH_4^+, in addition to upwelling (E2), was important during OAE 2. Thus, high lateral regional exchange may have contributed to a further decrease in $\delta^{15}N_{TN}$, especially in areas dominated by downwelling, such as the North-Eastern Coast and Central Open Ocean. The presence of N_2 fixers using an alternative nitrogenase enzyme in the water column and with significantly larger fractionations (−6 to −7‰) may have also contributed to the negative $\delta^{15}N_{TN}$ signal [*Zerkle et al.*, 2008; *Zhang et al.*, 2014]. However, in our sensitivity analysis (Figure 5), we find that a fractionation factor for N_2 fixation lower than −4‰ leads to a very negative $\delta^{15}N_{model}$. Such low values are not observed in the $\delta^{15}N_{TN}$. Instead, N_2 fixation and partial NH_4^+ uptake by phytoplankton may be of similar importance when considering a relatively small fractionation factor for both processes.

In the Southern Coast, all numerical experiments that consider a fractionation effect by primary production due to incomplete uptake of NH_4^+ (E2 and E3 performed with both models) capture the $\delta^{15}N_{TN}$ signal of the most negative values recorded during OAE 2 (Figure 6d). This suggests that upwelling rather than lateral input of NH_4^+ or N_2 fixation likely dominated the $\delta^{15}N_{TN}$ because inputs of NH_4^+ due to lateral fluxes and N_2 fixation do not significantly affect the $\delta^{15}N_{TN}$. This is best explained by the highly reducing conditions and is consistent with hypotheses of *Higgins et al.* [2012], based on records of $\delta^{15}N_{TN}$ at Demerara Rise.

Temporal variations in oxygen conditions may have occurred within the OAE 2 interval [e.g., *Hetzel et al.*, 2011] related to cooling (e.g., Plenus Cold Event) [*Gale and Christensen*, 1996] and may have been associated with changes in the depth of the chemocline. Periods of strong oxygen depletion may have first led to an increase in denitrification and N_2 fixation and thus primary production. As a consequence, oxygen further decreased in bottom waters (due to enhanced respiration), while NH_4^+ may have increased, as well as its vertical and lateral transport. This would have affected not only the area where NH_4^+ was being produced (such as the Southern Coast) but also areas where conditions were less reducing, such as the Northern Coast. This may explain the high variability observed in most $\delta^{15}N_{TN}$ records, especially at Bass River, Wunstorf, and site 1276 (Figures 3 and 4). At Bass River, which is a shallow coastal site, the largest variability may also be linked to high riverine influence [*van Helmond et al.*, 2014a], while at Wunstorf this may be associated with large changes in water column redox conditions.

Acknowledgments
Special thanks to José Mogollón Lee and Robin P.M. Topper for useful discussions that helped improve the model and interpretation of results. We would like to thank Christopher Junium and an anonymous reviewer for their useful comments. This research was funded by a Focus and Massa project granted to C.P. Slomp and H. Brinkhuis by Utrecht University and by the European Research Council under the European Community's Seventh Framework Program, ERC Starting grant 278364. Additional financial support was provided by Statoil and the Netherlands Earth System Science Centre. New data of $\delta^{15}N$ are available in Data Publisher for Earth and Environmental Science (PANGEA), and model code can be requested by sending an email to the corresponding author.

6. Summary

Our compilation of $\delta^{15}N_{TN}$ values from the literature and from five new sites presented in this study highlights a consistent shift of $\delta^{15}N_{TN}$ to lighter values during OAE 2 with a distinct lower limit of −3‰. We find large regional differences in the magnitude of this shift with the largest shift being observed in the Central Open Ocean and a relatively minor one at more oxygenated coastal sites. Box model results for N dynamics indicate that enhanced N_2 fixation likely explains most of the shift in $\delta^{15}N_{TN}$. Upwelling of NH_4^+ was likely of additional importance along the Southern Coast of the proto-North Atlantic, linked to the presence of highly reducing bottom waters. Lateral transport of NH_4^+ may also have contributed to the $\delta^{15}N_{TN}$ at many locations. The high temporal variability in $\delta^{15}N_{TN}$ may be the result of waxing and waning of the low-oxygen conditions, leading to temporal variations in N_2 fixation and NH_4^+ supply.

References

Algeo, T. J., P. A. Meyers, R. S. Robinson, H. Rowe, and G. Q. Jiang (2014), Icehouse-greenhouse variations in marine denitrification, *Biogeosciences*, *11*(4), 1273–1295.

Altabet, M. A., and R. Francois (1994), Sedimentary nitrogen isotopic ratio as a recorder for surface ocean nitrate utilization, *Global Biogeochem. Cycles*, *8*(1), 103–116, doi:10.1029/93GB03396.

Bauersachs, T., S. Schouten, J. Compaoré, U. Wollenzien, L. J. Stal, and J. S. Sinninghe Damsté (2009), Nitrogen isotopic fractionation associated with growth on dinitrogen gas and nitrate by cyanobacteria, *Limnol. Oceanogr.*, *54*(4), 1403–1411.

Blumenberg, M., and F. Wiese (2012), Imbalanced nutrients as triggers for black shale formation in a shallow shelf setting during the OAE 2 (Wunstorf, Germany), *Biogeosciences*, *9*, 4139–4153.

Bowman, A. R., and T. J. Bralower (2005), Paleoceanographic significance of high-resolution carbon isotope records across the Cenomanian-Turonian boundary in the Western Interior and New Jersey coastal plain, USA, *Mar. Geol.*, *217*, 305–321.

Brandes, J. A., and A. H. Devol (1997), Isotopic fractionation of oxygen and nitrogen in coastal marine sediments, *Geochim. Cosmochim. Acta*, *61*(9), 1793–1801.

Brandes, J. A., and A. H. Devol (2002), A global marine-fixed nitrogen isotopic budget: Implications for Holocene nitrogen cycling, *Global Biogeochem. Cycles*, *16*(4), 1120, doi:10.1029/2001GB001856.

Brodie, C. R., M. J. Leng, J. S. L. Casford, C. P. Kendrick, J. M. Lloyd, Z. Yongqiang, and M. I. Bird (2011), Evidence for bias in C and N concentrations and δ^{13}C composition of terrestrial and aquatic organic materials due to pre-analysis acid preparation methods, *Chem. Geol.*, *282*(3), 67–83.

Brunner, B., et al. (2013), Nitrogen isotope effects induced by anammox bacteria, *Proc. Natl. Acad. Sci.*, *110*(47), 18,994–18,999.

Capone, D. G., J. P. Zehr, H. W. Paerl, B. Bergman, and E. J. Carpenter (1997), Trichodesmium, a globally significant marine cyanobacterium, *Science*, *276*(5316), 1221–1229.

Carpenter, E. J., H. R. Harvey, B. Fry, and D. G. Capone (1997), Biogeochemical tracers of the marine cyanobacterium Trichodesmium, *Deep Sea Res., Part I*, *44*(1), 27–38.

Codispoti, L. A., J. A. Brandes, J. P. Christensen, A. H. Devol, S. W. A. Naqvi, H. W. Paerl, and T. Yoshinari (2001), The oceanic fixed nitrogen and nitrous oxide budgets: Moving targets as we enter the anthropocene?, *Sci. Mar.*, *65*(S2), 85–105.

Deutsch, C., D. M. Sigman, R. C. Thunell, A. N. Meckler, and G. H. Haug (2004), Isotopic constraints on glacial/interglacial changes in the oceanic nitrogen budget, *Global Biogeochem. Cycles*, *18*, GB4012, doi:10.1029/2003GB002189.

Devol, A. H. (2003), Nitrogen cycle: Solution to a marine mystery, *Nature*, *422*(6932), 575–576.

Du Vivier, A. D., D. Selby, B. B. Sageman, I. Jarvis, D. R. Gröcke, and S. Voigt (2014), Marine ^{187}Os/^{188}Os isotope stratigraphy reveals the interaction of volcanism and ocean circulation during Oceanic Anoxic Event 2, *Earth Planet. Sci. Lett.*, *389*, 23–33.

Gale, A. S., and W. K. Christensen (1996), Occurrence of the belemnite Actinocamax plenus in the Cenomanian of SE France and its significance, *Bull. Geol. Soc. Den.*, *43*, 68–77.

Ganeshram, R. S., T. F. Pedersen, S. Calvert, and R. François (2002), Reduced nitrogen fixation in the glacial ocean inferred from changes in marine nitrogen and phosphorus inventories, *Nature*, *415*(6868), 156–159.

Granger, J., D. M. Sigman, M. F. Lehmann, and P. D. Tortell (2008), Nitrogen and oxygen isotope fractionation during dissimilatory nitrate reduction by denitrifying bacteria, *Limnol. Oceanogr.*, *53*(6), 2533–2545.

Gruber, N. (2004), The dynamics of the marine nitrogen cycle and its influence on atmospheric CO_2 variations, in *The Ocean Carbon Cycle and Climate*, pp. 97–148, Springer, Netherlands.

Hetzel, A., C. März, C. Vogt, and H.-J. Brumsack (2011), Geochemical environment of Cenomanian-Turonian black shale deposition at Wunstorf (northern Germany), *Cretaceous Res.*, *32*, 480–494.

Higgins, M. B., F. Wolfe-Simon, R. S. Robinson, Y. Qin, M. A. Saito, and A. Pearson (2011), Paleoenvironmental implications of taxonomic variation among δ^{15}N values of chloropigments, *Geochim. Cosmochim. Acta*, *75*(22), 7351–7363.

Higgins, M. B., R. S. Robinson, J. M. Husson, S. J. Carter, and A. Pearson (2012), Dominant eukaryotic export production during ocean anoxic events reflects the importance of recycled NH_{4+}, *Proc. Natl. Acad. Sci.*, *109*(7), 2269–2274.

Hoch, M. P., M. L. Fogel, and D. L. Kirchman (1992), Isotope fractionation associated with ammonium uptake by a marine bacterium, *Limnol. Oceanogr.*, *37*(7), 1447–1459, doi:10.4319/lo.1992.37.7.1447.

Hoch, M. P., M. L. Fogel, and D. L. Kirchman (1994), Isotope fractionation during ammonium uptake by marine microbial assemblages, *Geomicrobiol. J.*, *12*(2), 113–127.

Jenkyns, H. C., A. Matthews, H. Tsikos, and Y. Erel (2007), Nitrate reduction, sulfate reduction, and sedimentary iron isotope evolution during the Cenomanian-Turonian Oceanic Anoxic Event, *Paleoceanography*, *22*, PA3208, doi:10.1029/2006PA001355.

Junium, C. K., and M. A. Arthur (2007), Nitrogen cycling during the Cretaceous, Cenomanian-Turonian Oceanic Anoxic Event II, *Geochem. Geophys. Geosyst.*, *8*(3), 1–18, doi:10.1029/2006GC001328.

Junium, C. K., K. H. Freeman, and M. A. Arthur (2014), Controls on the stratigraphic distribution and nitrogen isotopic composition of zinc, vanadyl and free base porphyrins through Oceanic Anoxic Event 2 at Demerara Rise, *Org. Geochem.*, *80*, 60–71.

Kritee, K., D. M. Sigman, J. Granger, B. B. Ward, A. Jayakumar, and C. Deutsch (2012), Reduced isotope fractionation by denitrification under conditions relevant to the ocean, *Geochim. Cosmochim. Acta*, *92*, 243–259.

Kuypers, M. M. M., R. D. Pancost, I. A. Nijenhuis, and J. S. Sinninghe Damsté (2002), Enhanced productivity led to increased organic carbon burial in the euxinic North Atlantic basin during the late Cenomanian Oceanic Anoxic Event, *Paleoceanography*, *17*(4), 1051, doi:10.1029/2000PA000569.

Kuypers, M. M. M., Y. van Breugel, S. Schouten, E. Erba, and J. S. Sinninghe Damsté (2004), N_2-fixing cyanobacteria supplied nutrient N for Cretaceous Oceanic Anoxic Events, *Geology*, *32*(10), 853–856.

Lohse, L., R. T. Kloosterhuis, H. C. de Stigter, W. Helder, W. van Raaphorst, and T. C. van Weering (2000), Carbonate removal by acidification causes loss of nitrogenous compounds in continental margin sediments, *Mar. Chem.*, *69*(3), 193–201.

Mariotti, A., J. C. Germon, P. Hubert, P. Kaiser, R. Letolle, A. Tardieux, and P. Tardieux (1981), Experimental determination of nitrogen kinetic isotope fractionation: Some principles; illustration for the denitrification and nitrification processes, *Plant Soil*, *62*(3), 413–430.

Middelburg, J. J., K. Soetaert, P. M. J. Herman, and C. H. R. Heip (1996), Denitrification in marine sediments: A model study, *Global Biogeochem. Cycles*, *10*(4), 661–673.

Möbius, J., N. Lahajnar, and K.-C. Emeis (2010), Diagenetic control of nitrogen isotope ratios in Holocene sapropels and recent sediments from the Eastern Mediterranean Sea, *Biogeosciences*, *7*, 3901–3914.

Monteiro, F. M., R. D. Pancost, A. Ridgwell, and Y. Donnadieu (2012), Nutrients as the dominant control on the spread of anoxia and euxinia across the Cenomanian-Turonian Oceanic Anoxic Event (OAE2): Model-data comparison, *Paleoceanography*, *27*, PA4209, doi:10.1029/2012PA002351.

Nieuwenhuize, J., Y. E. M. Maas, and J. J. Middelburg (1994), Rapid analysis of organic carbon and nitrogen in particulate materials, *Mar. Chem.*, *45*(3), 217–224.

Owens, J. D., T. W. Lyons, X. Li, K. G. Macleod, G. Gordon, M. M. M. Kuypers, A. Anbar, W. Kuhnt, and S. Severmann (2012), Iron isotope and trace metal records of iron cycling in the proto-North Atlantic during the Cenomanian-Turonian Oceanic Anoxic Event (OAE-2), *Palaeogeography*, *27*, PA3223, doi:10.1029/2012PA002328.

Rau, G. H., M. A. Arthur, and W. E. Dean (1987), $^{15}N/^{14}N$ variations in Cretaceous Atlantic sedimentary sequences: Implication for past changes in marine nitrogen biogeochemistry, *Earth Planet. Sci. Lett.*, *82*(3), 269–279.

Robinson, R. S., et al. (2012), A review of nitrogen isotopic alteration in marine sediments, *Paleoceanography*, *27*, PA4203, doi:10.1029/2012PA002321.

Ruvalcaba Baroni, I., R. P. M. Topper, N. A. G. M. van Helmond, H. Brinkhuis, and C. P. Slomp (2014a), Biogeochemistry of the North Atlantic during Oceanic Anoxic Event 2: Role of changes in ocean circulation and phosphorus input, *Biogeosciences*, *11*(4), 977–993.

Ruvalcaba Baroni, I., I. Tsandev, and C. P. Slomp (2014b), Enhanced N_2-fixation and NH_4^+ recycling during Oceanic Anoxic Event 2 in the proto-North Atlantic, *Geochem. Geophys. Geosyst.*, *15*, 4064–4078, doi:10.1002/2014GC005453.

Ryabenko, E. (2013), Stable isotope methods for the study of the nitrogen cycle, in *Topics in Oceanography*, edited by E. Zambianchi, InTech., doi:10.5772/56105. [Available from http://www.intechopen.com/books/topics-in-oceanography/stable-isotope-methods-for-the-study-of-the-nitrogen-cycle.]

Sinninghe Damsté, J. S., and J. Köster (1998), A euxinic southern North Atlantic Ocean during the Cenomanian-Turonian Oceanic Anoxic Event, *Earth Planet. Sci. Lett.*, *158*, 165–173.

Sinninghe Damsté, J. S., E. C. van Bentum, G.-J. Reichart, P. Pross, and S. Schouten (2010), A CO_2 decrease-driven cooling and increased latitudinal temperature gradient during the mid-Cretaceous Oceanic Anoxic Event 2, *Earth Planet. Sci. Lett.*, *293*(1–2), 97–103.

Sugarman, P. J., K. G. Miller, R. K. Olsson, J. V. Browning, J. D. Wright, L. M. de Romero, T. S. White, F. L. Muller, and J. Uptegrove (1999), The Cenomanian-Turonian carbon burial event, Bass River, NJ, USA: Geochemical, paleoecological, and sea-level changes, *J. Foraminiferal Res.*, *29*, 438–452.

Tsikos, H., et al. (2004), Carbon-isotope stratigraphy recorded by the Cenomanian-Turonian Oceanic Anoxic Event: Correlation and implications based on three key localities, *J. Geol. Soc.*, *161*(4), 711–719.

Urquhart, E., S. Gardin, R. M. Leckie, S. A. Wood, J. Pross, M. D. Georgescu, B. Ladner, and H. Takata (2007), A paleontological synthesis of ODP Leg 210, Newfoundland Basin, in *Proceedings of ODP, Scientific Results, 210*, edited by B. E. Tucholke, J. C. Sibuet, and A. Klaus, pp. 1–53, Ocean Drilling Program, College Station, Tex.

van Bentum, E. C., G.-J. Reichart, and J. S. Sinninghe Damsté (2012), Organic matter provenance, palaeoproductivity and bottom water anoxia during the Cenomanian/Turonian Oceanic Anoxic Event in the Newfoundland Basin (northern proto North Atlantic Ocean), *Org. Geochem.*, *50*, 11–18.

van Helmond, N. A. G. M., A. Sluijs, G.-J. Reichart, J. S. Sinninghe Damsté, C. P. Slomp, and H. Brinkhuis (2014a), A perturbed hydrological cycle during Oceanic Anoxic Event 2, *Geology*, *42*(2), 123–126.

van Helmond, N. A. G. M., I. Ruvalcaba Baroni, A. Sluijs, J. S. Sinninghe Damsté, and C. P. Slomp (2014b), Spatial extent and degree of oxygen depletion in the deep proto-North Atlantic basin during Oceanic Anoxic Event 2, *Geochem. Geophys. Geosyst.*, *15*(11), 4254–4266, doi:10.1002/2014GC005528.

van Helmond, N. A. G. M., A. Sluijs, J. S. Sinninghe Damsté, G.-J. Reichart, S. Voigt, J. Erbacher, J. Pross, and H. Brinkhuis (2015), Freshwater discharge controlled deposition of Cenomanian-Turonian black shales on the NW European epicontinental shelf (Wunstorf, North Germany), *Clim. Past*, *11*, 495–508, doi:10.5194/cp-11-495-2015.

Voigt, S., J. Erbacher, J. Mutterlose, W. Weiss, T. Westerhold, F. Wiese, M. Wilmsen, and T. Wonik (2008), The Cenomanian-Turonian of the Wunstorf section-(North Germany): Global stratigraphic reference section and new orbital time scale for Oceanic Anoxic Event 2, *Newslett. Stratigr.*, *43*(1), 65–89.

Waser, N. A. D., P. J. Harrison, B. Nielsen, S. E. Calvert, and D. H. Turpin (1998), Nitrogen isotope fractionation during the uptake and assimilation of nitrate, nitrite, ammonium, and urea by a marine diatom, *Limnol. Oceanogr.*, *43*(2), 215–224.

Wilmsen, M. (2003), Sequence stratigraphy and palaeoceanography of the Cenomanian Stage in northern Germany, *Cretaceous Res.*, *24*(5), 525–568.

Zerkle, A. L., C. K. Junium, D. E. Canfield, and C. H. House (2008), Production of ^{15}N-depleted biomass during cyanobacterial N_2-fixation at high Fe concentrations, *J. Geophys. Res.*, *113*, 1–9, doi:10.1029/2007JG000651.

Zhang, X., D. M. Sigman, F. M. M. Morel, and A. M. L. Kraepiel (2014), Nitrogen isotope fractionation by alternative nitrogenases and past ocean anoxia, *Proc. Natl. Acad. Sci.*, *111*(13), 4782–4787.